Received: 6 July 2022 | Revised: 25 October 2022 | Accepted: 27 October 2022

DOI: 10.1002/alz.12886

Alzheimer's & Dementia®
THE JOURNAL OF THE ALZHEIMER'S ASSOCIATION

FEATURED ARTICLE

Quantification of [^{18}F]florbetaben amyloid-PET imaging in a mixed memory clinic population: The ABIDE project

Lyduine E. Collij[1] | **Gemma Salvadó**[2,3] | **Arno de Wilde**[4] | **Daniele Altomare**[5,6] | **Mahnaz Shekari**[2,7,8] | **Juan Domingo Gispert**[2,7,9] | **Santiago Bullich**[10] | **Andrew Stephens**[10] | **Frederik Barkhof**[1,11] | **Philip Scheltens**[4] | **Femke Bouwman**[4] | **Wiesje M. van der Flier**[4,12]

[1]Department of Radiology and Nuclear Medicine, Amsterdam University Medical Center, Amsterdam Neuroscience, Amsterdam, The Netherlands

[2]Barcelonaβeta Brain Research Center (BBRC), Pasqual Maragall Foundation, Barcelona, Spain

[3]Clinical Memory Research Unit, Department of Clinical Sciences, Lund University, Malmö, Sweden

[4]Department of Neurology, Alzheimer Center Amsterdam, Amsterdam Neuroscience, Vrije Universiteit Amsterdam, Amsterdam UMC, Amsterdam, The Netherlands

[5]Laboratory of Neuroimaging of Aging (LANVIE), University of Geneva, Geneva, Switzerland

[6]Memory Center, Geneva University Hospitals, Geneva, Switzerland

[7]IMIM (Hospital del Mar Medical Research Institute), Barcelona, Spain

[8]Pompeu Fabra University, Barcelona, Spain

[9]Centro de Investigación Biomédica en Red de Bioingeniería, Biomateriales y Nanomedicina (CIBER-BBN), Madrid, Spain

[10]Life Molecular Imaging GmbH, Berlin, Germany

[11]Centre for Medical Image Computing, and Queen Square Institute of Neurology, UCL, London, UK

[12]Department of Epidemiology & Data Science, Amsterdam Neuroscience, Vrije Universiteit Amsterdam, Amsterdam UMC, Amsterdam, The Netherlands

Correspondence
Lyduine E. Collij, Department of Radiology and Nuclear Medicine, Amsterdam University Medical Center, Amsterdam Neuroscience, PK -1×014, 1182 DB, Amsterdam, The Netherlands.
Email: l.collij@amsterdamumc.nl

Funding information
Life Molecular Imaging GmbH, Grant/Award Number: LSHM18075; ZonMW, Grant/Award Number: #73305095007; Topsector Life Sciences & Health, Grant/Award Number: #LSHM20106; Dutch national dementia plan, Grant/Award Number: 733050201; Innovative Medicines Initiative 2 Joint Undertaking, Grant/Award Number: 115952

Abstract

Introduction: We investigated amyloid-burden quantification in a mixed memory clinic population.

Methods: [^{18}F]Florbetaben amyloid-PET (positron emission tomography) scans of 348 patients were visually read and quantified using the Centiloid (CL) method. General linear models were used to assess CL differences across syndromic and etiological diagnosis. Linear mixed models were fitted to assess the predictive value of visual read (VR) and CL on longitudinal Mini-Mental Status Examination (MMSE).

Results: CL was associated with syndromic (F = 4.42, p = 0.014) and etiological diagnosis (F = -12.66, p < 0.001), with Alzheimer's disease (AD) patients showing the highest amyloid burden (62.9 ± 27.5), followed by dementia with Lewy bodies (DLB) (25.3 ± 35.5) and cardiovascular disease (CVD) (16.7 ± 24.5), and finally frontotemporal lobe degeneration (FTLD) (5.0 ± 17.22, t = −12.66, p < 0.001). CL remained predictive of etiological diagnosis (t = −2.41, p = 0.017) within the VR+ population

($N = 157$). VR was not a significant predictor of MMSE ($t = -1.53$, $p = 0.13$) for the SCD population ($N = 90$), whereas CL was ($t = -3.30$, $p = 0.001$).

Discussion: The extent of amyloid pathology through quantification holds clinical value, potentially in the context of differential diagnosis as well as prognosis.

KEYWORDS
Amyloid-PET, Centiloid quantification, Dementia, Diagnosis, Prognosis

1 | INTRODUCTION

Amyloid positron emission tomography (PET) imaging allows the in vivo visualization and quantification of the amyloid-beta (Aβ) protein, a pathological hallmark of Alzheimer's disease (AD).[1] In a clinical setting, amyloid-PET images are visually assessed by trained readers, resulting in a binary classification of negative or positive for the presence of fibrillary Aβ in the brain.[2] This rather straightforward approach has shown clinical value, with several studies including the Alzheimer Biomarkers in Daily Practice (ABIDE)-PET study demonstrating an increase in diagnostic confidence and change in patient diagnosis and management after amyloid-PET.[3–5] However, quantifying the extent of pathology could support the identification of emerging or focal pathology,[6–8] provide prognostic information,[7,9,10] and has possibly differential diagnostic utility. It is therefore of interest to assess the potential value of amyloid quantification in a memory clinic cohort to optimize the utility of amyloid-PET imaging.

Quantification is suggested to support reliable identification of amyloid pathological burden and reflect its extent.[7,11,12] A commonly implemented quantification approach is the Centiloid (CL) method,[13] which brings the tracer-specific standard uptake value ratio (SUVr) metric to a standardized scale, effectively providing a generalizable measure of amyloid burden. Specifically for CL, neuropathological studies have shown that the earliest detectable amyloid PET signal occurs around 12 CL, whereas 19 to 24 CL best discriminates between subjects with none-to-low Aβ plaque burden and those with intermediate-to-high deposition.[14–16]

On the other end of the spectrum, a CL burden of >50 seems best to confirm a clinicopathological diagnosis of AD,[15] and the average burden of patients with AD dementia can vary from 84 CL[17] to 100 CL.[13] Although traditional visual read approaches do not seem to differentiate between distinct amyloid-positive disorders such as AD and dementia with Lewy bodies (DLB),[18] a recent publication suggests that patients with are positive for DLB had lower amyloid burden compared to their AD dementia counterparts.[19] Similarly, lower levels of amyloid burden are often observed in dementia patients with vascular burden.[20] Taken together, CL quantification provides a more fine-grained picture of pathological burden and could hold complementary information to visual assessments in the clinical routine for diagnosis.

However, most previous studies on the possible value of (CL) quantification in clinical populations have been performed in highly controlled research populations focused specifically on AD,[21,22] such as the Alzheimer's Disease Neuroimaging Initiative (ADNI) cohort, which are less reflective of daily clinical practice and therefore have limited generalizability. By contrast, the ABIDE study represents an unselected mixed memory clinic cohort, with a clinically relevant and heterogeneous patient population due to different underlying etiologies. It is conceivable that quantification would hold more value compared to binary visual reads, particularly in the context of assessing non-AD pathologies (such as DLB and cerebrovascular disease [CVD]). To date, little is known on CL measures in such real-life memory clinical populations.

To assess the potential value of quantification in clinical routine, we performed visual read and CL quantification of [^{18}F]florbetaben amyloid-PET images from an unselected mixed memory cohort, reflecting a heterogeneous clinical population including patients with AD and non-AD dementia, mild cognitive impairment (MCI), and subjective cognitive decline (SCD). First we investigated the agreement between the two measures across the whole cohort. Next, we determined whether CL burden was associated with syndromic and etiological diagnosis. Finally, we assessed the added value of CL quantification to visual read in predicting global cognitive decline across the three clinical groups.

2 | METHODS

2.1 | Cohort

The current work is based on data collected as part of the Alzheimer Biomarkers in Daily Practice (ABIDE) project, in which amyloid-PET was performed in 476 patients who visited the memory clinic of the Alzheimer Center Amsterdam VU University Medical Center (VUmc) between January 2015 and December 2016 and embedded into the routine diagnostic workup.[3,23] All patients underwent a standard diagnostic dementia evaluation that consisted of their medical and informant-based history as well as results from neurological examinations, neuropsychological testing, basic laboratory testing, and magnetic resonance imaging (MRI).[24] Clinical stage (SCD, MCI, or dementia), and the suspected primary etiology (AD, CVD, frontotemporal lobe degeneration [FTLD], DLB, other neurodegenerative disease [other ND], or non-neurodegenerative [non-ND]) were determined during multidisciplinary meetings. Next, visual read amyloid-PET results were

TABLE 1 Demographics

	All ($N = 348$)	SCD ($N = 130$)	MCI ($N = 63$)	Dementia ($N = 155$)
Age, years	64.3 (8.0)	60.7 (8.0)	66.3 (7.0)	66.6 (7.3)
Sex (F)	142 (40.8%)	56 (43.1%)	22 (34.9%)	64 (41.3%)
MMSE	25.6 (3.9)	27.7 (2.4)	26.8 (2.2)	23.2 (4.1)
Primary etiological diagnosis	AD: 140 (40.2%) Vascular: 17 (4.9%) FTLD: 30 (8.6%) DLB: 21 (6.0%) Other ND: 18 (5.2%) Not ND: 122 (35.1%)	AD: 22 (16.9%) Vascular: 3 (2.3%) FTLD: 1 (0.8%) DLB: 1 (0.8%) Other ND: 2 (1.5%) Not ND: 101 (77.7%)	AD: 33 (52.4%) Vascular: 4 (6.3%) FTLD: 5 (7.9%) DLB: 1 (1.6%) Other ND: 1 (1.6%) Not ND: 19 (30.2%)	AD: 85 (54.8%) Vascular: 10 (6.5%) FTLD: 24 (15.5%) DLB: 19 (12.3%) Other ND: 15 (9.7%) Not ND: 2 (1.3%)
APOE ε4 carrier	162 (46.6%)	51 (39.2%)	29 (46.0%)	82 (52.9%)
VR+	157 (45.1%)	26 (20.0%)	32 (50.8%)	99 (63.9%)
Centiloid	29.5 (36.3)	13.3 (26.4)	29.7 (34.0)	43.0 (38.8)
Centiloid stages	Negative: 179 (51.4%) uncertain: 19 (5.5%) Moderate: 40 (11.5%) High: 51 (14.7%) Very high: 59 (17.0%)	Negative: 96 (73.8%) uncertain: 5 (3.8%) Moderate: 16 (12.3%) High: 6 (4.6%) Very high: 7 (5.4%)	Negative: 30 (47.6%) uncertain: 6 (9.5%) Moderate: 5 (7.9%) High: 17 (27.0%) Very high: 5 (7.9%)	Negative: 53 (34.2%) uncertain: 8 (5.2%) Moderate: 19 (12.3%) High: 28 (18.1%) Very high: 47 (30.3%)

Abbreviations: SCD, subjective cognitive decline; MCI , mild cognitive impairment; MMSE, Mini-Mental State Examination; VR, visual read; CL, Centiloid; AD, Alzheimer's disease; FTLD, frontotemporal lobe degeneration; DLB, dementia with Lewy bodies; ND, neurodegeneration. Centiloid stages: CL: <15 CL, negative; 15 to 25 CL, uncertain; 26 to 50 CL, moderate; 51 to 75 CL, high; and >75 CL, very high.

disclosed to the neurologists, who reevaluated the clinical stage, suspected etiological diagnosis, and patient treatment. In this follow-up work, the final diagnosis documented after disclosure of the amyloid-PET results was used.[3] The medical ethics review committees of the VUmc approved the study. Informed consent was obtained from all individual participants included in the study.

2.2 | Participants

From the ABIDE-PET sample, 348 patients had a PET acquisition of sufficient quality (see below) for quantification purposes and were included in the current study. The final sample included 130 (37.4%) patients with SCD, 63 (18.1%) with MCI, and 155 (44.5%) with dementia. The prevalence of an AD etiological diagnosis was 16.9% ($N = 22$) in SCD, 52.4% ($N = 33$) in MCI, and 54.8% ($N = 85$) in patients with dementia. A primary non-AD etiological diagnosis was most often FTLD ($N = 24$, 15.5%) and DLB ($N = 19$, 12.3%) in patients with dementia, whereas a non-neurodegenerative disorder (e.g., psychiatric) was more prevalent in SCD ($N = 101$, 77.7%) and MCI ($N = 19$, 30.2%) (Table 1).

2.3 | PET acquisition and quantification

PET scans were obtained on a 3 Tesla Philips Ingenuity TF PET/MR or Philips Gemini TF PET/CT scanner. Both scanners had an effective resolution of 6.1 mm based on Hoffman-Phantom acquisition; thus no further harmonization steps were implemented. As per standard protocol, 20 minute scans consisting of 4 × 5 minute frames were collected 90 to 110 minutes post-injection of ≈300 MBq ± 20% [^{18}F]florbetaben (Neuraceq, Life Molecular Imaging, Berlin, Germany). Image reconstruction was done by applying the line of response row-action maximum likelihood (LOR-RAMLA) algorithm for the brain using default smoothing parameters.[25] Prior to the PET scan, a T1-weighted gradient echo pulse MRI or low-dose CT scan was acquired for attenuation correction of the PET data. To make sure the PET data were of sufficient quality for quantification purposes, all scans were manually checked for inter- and intra-frame motion and large lesions. In addition, a T1-weighted image of sufficient quality within 6 months of PET acquisition was required.

All scans were pre-processed using a validated standard CL pipeline and converted to the CL scale.[13] Briefly the four frames from the PET

images were first averaged and co-registered to the corresponding T1-weighted scans. Then the T1- weighted MRI scans were warped to standard space; the same warp was applied to warp the co-registered PET image. These procedures were performed in SPM12. PET images were intensity normalized using the whole cerebellum as the reference region using the mask provided by the CL method[13] (http://www.gaain.org/centiloid-project). Global cortical CL values were calculated using the Centiloid cortical mask (standard GAAIN target region). Please see Supplementary Methods for the Centiloid calibration. In addition, scans were classified according to five stages of CL: <15 CL, negative; 15 to 25 CL, uncertain; 26 to 50 CL, moderate; 51 to 75 CL, high; and >75 CL, very high.[10]

2.4 | Visual assessment of PET images

All PET scans were assessed visually by a certified and experienced nuclear physician (B.vB.) blinded to clinical diagnosis. Images were scaled based on the total white matter signal and using gray color scaling. Transverse, sagittal, and coronal views were displayed using the software package Vinci 2.56. Images were rated as either *positive* (binding in one or more cortical brain region unilaterally) or *negative* (predominantly white matter uptake) according to criteria defined in the label by the manufacturer (Life Molecular Imaging).

2.5 | Statistical analysis

All statistical analyses were performed in R version 4.0.2 and significance was set at $p < 0.05$. Differences in sample characteristics between diagnostic groups were assessed by analysis of variance (ANOVA) and chi-square tests, as appropriate.

Using ANOVA, differences in CL values between visual read negative (VR–) and positive (VR+) groups and between VR+ diagnostic groups were assessed. Next, we derived the optimal CL threshold using VR as standard of truth in a receiver-operating characteristic (ROC) analysis, maximizing the Youden's J Index.[26] Subsequently, we determined the number of discordant patients utilizing the optimal CL cutoff and assessed whether discordant patients differed in apolipoprotein E (*APOE*) ε4 carriership, age, and clinical stage compared to concordant patients.

Then, we investigated whether CL burden was related to primary etiology diagnostic groups using generalized linear models (GLMs), correcting for age, sex, *APOE* ε4 carriership, and clinical stage. GLM was repeated within the VR+ group only.

Finally, we determined whether the two measures of amyloid burden (i.e., VR and CL) predicted global cognitive decline as measured with the Mini-Mental State Examination (MMSE). In total, 218 subjects had longitudinal MMSE scores available, with a mean follow-up time of 3.0 years (SD = 1.2, range = 1.0 to 6.2). Linear mixed models with random intercept and slope were fitted, first for the whole cohort and subsequently stratified per clinical stage (i.e., SCD, MCI, and dementia). Predictors were the interaction between follow-up time and VR status (model 1), continuous CL (model 2), CL stages (model 3), and CL groups (model 4), where the latter reflects binary assignment of positivity based on the optimal CL cutoff derived from the ROC analysis. Covariates were age at baseline, sex, and clinical stage (only for the whole cohort) or etiological diagnosis in case of stratified analysis.

2.6 | Data availability

The data sets analyzed during the current study are available from the corresponding author on reasonable request.

3 | RESULTS

Demographics are presented in Table 1. Across the sample of 348 memory clinic patients, mean age was 64.3 (± 8.0), 142 (40.8%) were female, 162 (46.6%) were *APOE* ε4 carriers, and 157 (45.1%) were considered amyloidpositive based on VR. Mean age was lower for SCD (60.7 ± 8.0, $p < 0.001$), whereas MCI (66.3 ± 7.0) and dementia patients (mean = 66.6 ± SD = 7.3) did not differ ($p = .80$). The proportion of VR positivity increased with disease severity (SCD = 20.0%; MCI = 50.8%; dementia = 63.9%, $\chi^2 = 55.96$, $p < 0.001$). Amyloid burden as expressed in CL units was 29.5 on average (± 36.3, range = −27.8 to −122.0) and related to disease severity (SCD: 13.3 ± 26.4; MCI: 29.7 ± 34.0; dementia: 43.4 ± 38.8, $F = 27.3$, $p < 0.001$). Based on the pre-defined CL stages, 179 patients (51.4%) were classified as amyloid negative, 19 (5.5%) with low, 40 (11.5%) moderate, 51 (14.7%) high, and 59 (17.0%) very high amyloid burden. Patients with dementia due to AD were more often female ($N = 45$, 52.9%) and *APOE* ε4 carriers ($N = 62$, 72.9%) compared to their non-AD counterparts (sex: $N = 19$, 26.8%, $\chi^2 = 10.95$, $p < 0.001$; *APOE*: $N = 20$, 29.4%, $\chi^2 = 28.78$, $p < 0.001$), but did not differ in mean age.

3.1 | Visual assessment against Centiloid quantification

Amyloid positivity based on VR was associated with a higher CL burden compared to visually negative patients images (VR−: 3.0 ± 14.2; VR+: 61.7 ± 27.9, $F = 624.3$, $p < 0.001$, Figure 1). Within VR+ patients, CL burden increased with disease severity (SCD: 51.5 ± 27.2; MCI: 54.8 ± 29.7 dementia: 66.6 ± 26.5, $F = 4.42$, $p = .014$). The optimal CL cutoff as indicated by the Youden index (VR reference) was CL = 21 ($J = 0.86$, area under the curve [AUC] = 0.958, 95% confidence interval [CI]: 0.935 to 0.981; sensitivity = 92.4%, specificity = 93.7%). Utilizing this cutoff, 24 (6.9%) patients were considered discordant between VR and CL, with 12 patients (50%) assessed as VR+ but with a CL below 21 (i.e., CL−) and 12 patients (50%) assessed as VR− and a CL value above 21 (i.e., CL+). Discordant patients were less often *APOE* ε4 carriers (25.0% vs 48.9%, $\chi^2 = 5.12$, $p = 0.024$) and older (mean = 68.4, SD = 8.5 vs 64.0, SD = 7.9, $U = 2540$, $p = 0.005$). VR+/CL− patients were mainly patients with cognitive impairment

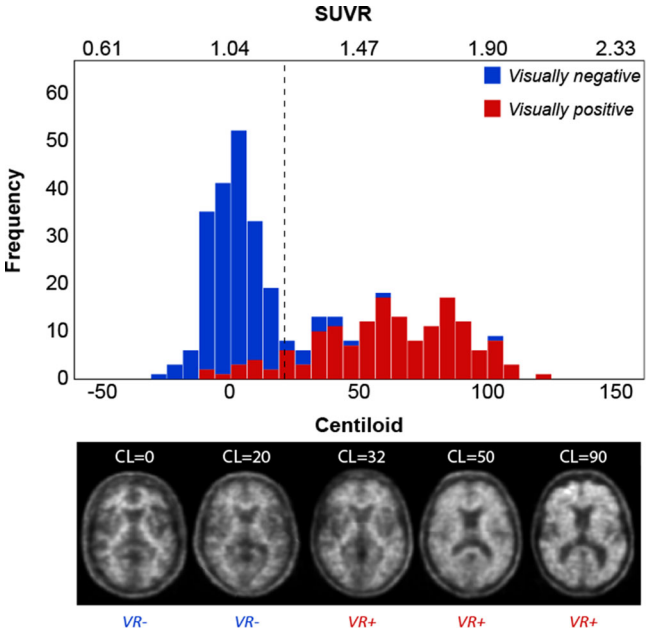

FIGURE 1 Centiloid distribution against visual assessment. Histogram displaying the frequency of Centiloid values color coded for visual read (VR) status. A bimodal distribution can be appreciated. Dashed line illustrates the optimal CL cutoff compared to VR as determined by the receiver-operating characteristic (ROC) analyses (i.e., CL = 21). Below some illustrative [^{18}F]florbetaben scans are shown across the continuum. SUVR = standard uptake value ratio

TABLE 2 Proportion of syndromic and etiological diagnosis stratified for visual read status

	Visually read negative		
	SCD $N = 104$	MCI $N = 31$	Dementia $N = 57$
AD	0 (0.0%)	1 (3.2%)	2 (3.5%)
Vascular	3 (2.9%)	4 (12.9%)	6 (10.5%)
FTLD	1 (1.0%)	5 (16.1%)	23 (40.4%)
DLB	1 (1.0%)	1 (3.2%)	9 (15.8%)
Other ND	2 (1.9%)	1 (3.2%)	14 (24.6%)
Not ND	97 (93.3%)	19 (61.3%)	3 (5.3%)
	Visually read positive		
	SCD $N = 26$	MCI $N = 32$	Dementia $N = 99$
AD	22 (84.6%)	32 (100%)	83 (83.3%)
Vascular	0 (0.0%)	0 (0.0%)	4 (4.0%)
FTLD	0 (0.0%)	0 (0.0%)	1 (1.0%)
DLB	0 (0.0%)	0 (0.0%)	10 (10.1%)
Other ND	0 (0.0%)	0 (0.0%)	1 (1.0%)
Not ND	4 (15.4%)	0 (0.0%)	0 (0.0%)

Abbreviations: SCD, subjective cognitive decline; MCI, mild cognitive impairment; MMSE, Mini-Mental State Examination; VR, visual read; CL, Centiloid; AD, Alzheimer's disease; FTLD, frontotemporal lobe degeneration; DLB, dementia with Lewy bodies; ND, neurodegeneration.

(SCD = 16.7%, MCI = 41.7%, dementia = 41.7%), whereas VR−/CL+ patients were either individuals with SCD or patients with dementia (SCD = 50.0%, MCI = 8.3%, dementia = 41.7%). See supplementary materials and Figure S1 for example of discordant cases. In general, CL−/VR+ positive cases often showed focal uptake in early accumulating regions (i.e., frontal or precuneus), whereas CL+/VR− cases were often assessed with a lower reader confidence due to possible temporal signal.

3.2 | Extent of amyloid pathology and primary etiological diagnosis

Most patients ($N = 188$, 98.4%) assessed as VR− had a primary non-AD etiological diagnosis, most often a non-neurodegenerative diagnosis ($N = 118$, 62.8%), followed by FTLD ($N = 28$, 15.4%), other neurodegenerative disorders ($N = 17$, 9.0%), CVD ($N = 13$, 6.9%), and DLB ($N = 11$, 5.9%). As expected, 137 (87.3%) of VR+ patients received a primary AD etiological diagnosis. The remaining VR+ patients were mostly patients with DLB ($N = 10$, 50.0%), CVD ($N = 4$, 20.0%), or considered to have SCDs without underlying neurodegeneration ($N = 4$, 20.0%), where an AD etiological diagnosis is less likely to be given (Table 2 and Figure S2).

The amount of amyloid pathology as expressed in CL units was associated with the primary etiological diagnosis after correcting for age, sex, *APOE* ε4 carriership, and clinical stage, with AD patients showing the highest amyloid burden (62.9 ± 27.5), followed by DLB (25.3 ± 35.5) and CVD (16.7 ± 24.5), and finally FTLD (5.0 ± 17.22, $t = -12.66$, $p < 0.001$, Figure 2). It is important to note that CL remained predictive of etiological diagnosis ($t = -2.41$, $p = 0.017$) within the VR+ population ($N = 157$), with mean CL burden being 64.1 (± 26.5) for AD patients, 44.3 (± 30.3) for CVD, and 49.9 (± 35.9) for DLB.

3.3 | Measures of amyloid to predict cognitive decline

To determine the predicted value of amyloid burden on global cognitive decline, four linear mixed models (LMMs) with different measures of pathological burden were fitted, namely binary VR status, continuous CL, CL stages (i.e., negative, uncertain, moderate, high, and very high), and CL groups (i.e., binary classification based on optimal ROC-derived cutoff of CL = 21). In the whole population with available repeated MMSE ($N = 218$), the interaction between VR and time was predictive of MMSE ($t = -4.63$, $p < 0.001$), corrected for age, sex, follow-up time, and clinical stage. CL models performed similarly to the VR model, with CL stages*time ($t = -4.96$, $p < 0.001$) and CL groups*time ($t = -5.12$, $p < 0.001$) being predictive of global cognitive decline. For the continuous CL model, both baseline CL units ($t = -1.99$, $p = 0.025$) and its interaction with time ($t = -4.59$, $p < 0.001$) were predictive of MMSE scores (Figure 3A).

After stratification for clinical stage, VR was not a significant predictor of global cognitive decline ($t = -1.53$, $p = .13$) for the SCD population

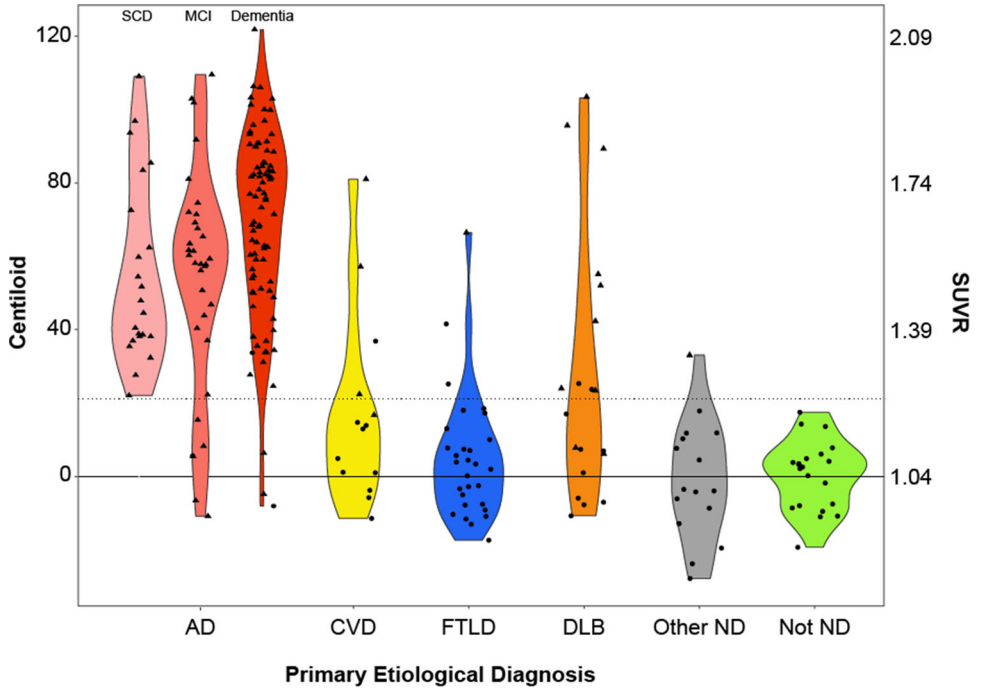

FIGURE 2 Centiloid burden across etiological diagnoses. Violin plot displaying the distribution of amyloid burden as measured in Centiloid units per primary etiological diagnosis. The AD population is further stratified based on clinical stage, showing a step-wise increase in amyloid burden. For the other diagnoses, data of only MCI and dementia patients are shown. The dotted line illustrates the optimal Youden index–based cutoff against visual read (CL = 21). Visually positive patients are shown as triangles, whereas visually negative patients are illustrated as circles. AD, Alzheimer's disease; CVD, cerebrovascular disease; FTLD, frontotemporal lobe degeneration; DLB, dementia with Lewy bodies; ND, neurodegeneration, SCD, subjective cognitive decline; MCI, mild cognitive impairment; SUVR, standard uptake value ratio

($N = 90$), whereas amyloid burden expressed in CL units*time had predictive value (continuous: $t = -3.30$, $p = 0.001$; CL stages: $t = -3.42$, $p < 0.001$; CL groups $t = -2.91$, $p = 0.005$). More specifically for the CL stages, only SCD subjects with high ($t = -3.10$, $p = 0.003$) or very high ($t = -2.69$, $p = 0.009$) amyloid burden showed steeper cognitive decline (Figure 3B). In MCI patients ($N = 48$), VR*time ($t = -3.22$, $p = 0.002$) and CL quantification*time (continuous: $t = -1.95$, $p = 0.05$, $\Delta AIC = -2.3$; CL stages: $t = -2.42$, $p = 0.02$; CL groups: $t = -3.28$, $p = 0.002$) performed similarly in predicting MMSE scores (Figure 3C). Finally, neither VR nor CL predicted further cognitive decline in patients with dementia ($N = 80$) or specifically non-AD dementia ($N = 37$).

4 | DISCUSSION

We illustrated the usefulness of quantification in a mixed memory clinic population compared to binary visual reads of amyloid-PET images, using the standardized Centiloid (or CL) method. We observed that CL quantification was in high agreement with VR status. In visually amyloid-positive subjects, the amount of pathology as expressed in CL units was associated with clinical stage and with primary etiological diagnosis, with AD patients showing the highest amyloid burden, followed by patients with DLB and CVD. Finally, although both VR and CL were predictive of global cognitive decline in MCI, CL quantification outperformed VR in participants with SCD. Together, these results support the added value of continuous assessments of amyloid pathology as measured with CL in clinical practice.

The high agreement between visual assessment and binary CL quantification is in line with previous literature, with excellent sensitivity and specificity reported across clinical disease stages.[6,14,27] The number of discordant VR/CL patients in this work was relatively low. This is probably due to the experience of the reader, who is highly familiar with assessing both clinically advanced scans[3,5] as well as those showing early amyloid pathology.[6] Indeed, previous work across different radiotracers illustrated that the accuracy and sensitivity of VR is highly dependent on reader experience, with less-experienced readers having the tendency to either assess frontal regions as positive in the absence of Aβ burden[28] or miss emerging pathology.[29] It is notable that the optimal CL cutoff compared to VR is remarkably consistent between the current work, post-mortem validation of [^{18}F]florbetaben CL quantification, and recent studies using either an experienced reader[14] or similar populations, despite differences in AD prevalence.[30] Quantification could, therefore, provide an objective measure to support visual assessment and reduce false-negative or false-positive classifications, especially for readers with less experience in detecting emerging or focal pathology.

In addition to supporting the detection of amyloid burden, quantification could also provide relevant information on the extent of pathology. As expected, the proportion of VR+ patients in this cohort increased from 20.0% in SCD to 63.9% in patients with demen-

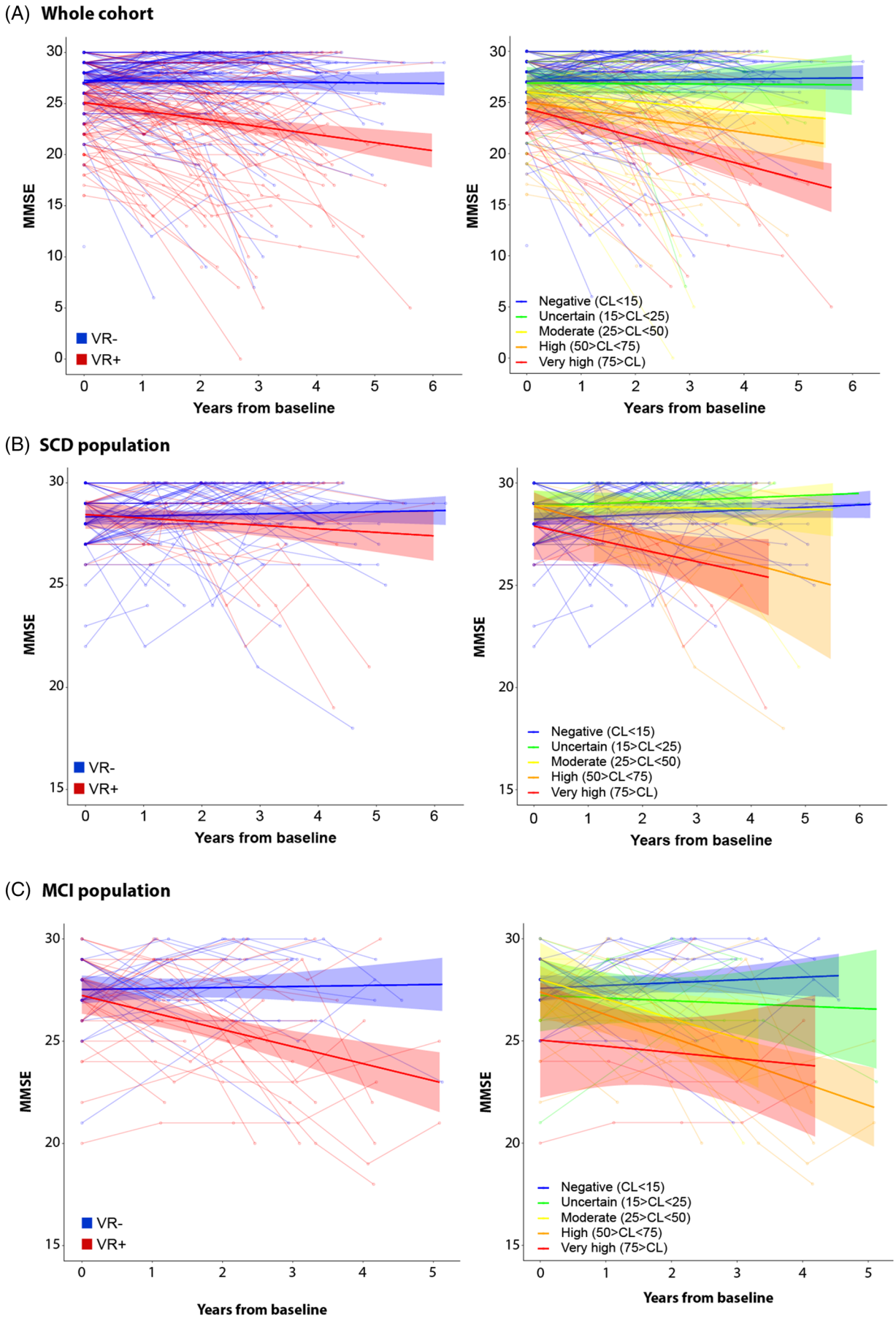

FIGURE 3 Measures of amyloid predict global cognitive decline. Results from the linear mixed model (LMM) analyses displaying the effect of baseline visual read (VR, left) and Centiloid stages (CL, right) on subsequent Mini-Mental State Examination (MMSE) scores with colored band representing the 95% confidence interval. (A) LMM results across diagnostic groups, showing similar performance of VR and CL quantification. (B) LMM results for the SCD population, for which VR was not a significant predictor of global cognitive decline, whereas CL was. Specifically, SCD subjects with CL > 50 have an increased risk of cognitive decline, which can be appreciated by the slope of the orange (high burden) and red (very

tia. However, visual amyloid-positivity was associated with a wide range of CL units across clinical stages, reflective of emerging[14] up to clinicopathological[13,15] levels of amyloid pathology in our clinically impaired patients. CL quantification was associated with the primary etiological diagnosis when corrected for clinical stage, with AD patients displaying the highest amyloid burden. This is line with previous work, where a clinicopathological cutoff (i.e., CL >50) associated with primary AD was proposed, whereas lower levels were considered indicative of amyloid as co-pathology.[14] Indeed, the mean burden in VR+ patients with DLB and CVD in this and previous[18,19] work support that observation. Of interest, although amyloid comorbidity is commonly observed in patients with dementia, no guidelines or criteria for identifying and recognizing mixed pathology exist. Our study provides the first step toward showing that quantification reflecting the amount of amyloid pathology, rather than dichotomization of amyloid burden, may hold value for describing mixed pathology and differential diagnostic information in memory clinic patients. Nonetheless, a portion of patients diagnosed with AD show CL values aligned with DLB. This was particularly the case for the MCI population, where Aβ burden is still accumulating and (Centiloid) quantification, therefore, has limited discriminative power between etiologies. In these cases, diagnosis could be further supported by tau-PET or fluorodeoxyglucose (FDG)-PET imaging. From a prognostic perspective, several studies have illustrated the value of continuous assessments to predict future cognitive decline, especially in early pre-symptomatic populations.[7,8,31] Consistent with those findings, we observed that in the SCD population, CL quantification was a better predictor of cognitive decline compared to VR, with a step-wise increased risk for the high and very high CL stages. One could take advantage of the standard CL measure and these findings to further characterize the A+ group within the ATN research framework.[1] Such an implementation would not only improve risk stratification for cognitive decline, but would also enable the identification of subjects most likely to benefit from disease-modifying interventions.[32,33] Especially in the context of (future) Aβ targeted therapies, quantification might even be required in future treatment decisions, such as treatment initiation, duration, and monitoring frequency.[34] Preparation of the field for this shift in the use of amyloid-PET and familiarizing its users with quantitative approaches is therefore key, and can be supported by several continuing education marketed software packages.[22]

Centiloid quantification has been shown to be a robust measure across multiple studies and cohort types. Its potential as a widely used clinical tool is further supported by recent work showing that major differences in pipeline design (e.g., analysis space, image resolution, tracer, and target VOI) minimally affect CL values, although use of the pons as reference region is discouraged as it results in significantly lower units.[35] However, conclusions on its possible clinical use are currently drawn from retrospective data. Future work is needed, therefore, to investigate whether quantitative amyloid-PET can further increase diagnostic confidence as well as impact patient management. Within the context of clinical implementation, it is important to note that interpretation of quantitation should always be performed in conjunction with a visual read to ensure data quality, understand possible causes of discordance, and consequently prevent false-negative and false-positive classifications based on CL. As illustrated by the discordant patients in this work, atrophy or focal uptake in regions less represented in the CL mask can result in lower values, whereas methodological issues such as suboptimal reference region delineation can cause inflated values. It is also important to note that a non-negligible portion of the ABIDE data set was not suitable for quantitation purposes, due to low image quality of either the PET or MR scan. This highlights the importance of proper staff training for data acquisition and processing, and the potential value of recently developed PET-only processing pipelines,[21,36] which could reduce the number of scans not suitable for quantification and further support clinical implementation.

The current work has some methodological considerations. First, a limitation of this study is its single-center design and consequently its lack of external validation. However, the heterogeneous composition, consisting of a real-life, memory clinic population is unique within the field, more adequately reflecting the mixed population assessed in clinical practice compared to other studies. Second, the relatively limited number of non-AD patients prohibited stratified longitudinal analyses of specific subpopulations. Collaboration with DLB or CVD cohorts could shed further light on the prognostic value of quantitative amyloid-PET for these important patient populations. Third, our

RESEARCH IN CONTEXT

1. **Systematic review**: Literature was reviewed using traditional sources (e.g., PubMed). Little is known about quantitative amyloid measures in a heterogeneous memory clinic population, while recent work has suggested the potential added value of such assessments.
2. **Interpretation**: Our findings suggest that quantification of amyloid burden through the Centiloid (CL) approach has potential diagnostic and prognostic value. In a mixed memory clinic cohort (Alzheimer Biomarkers in Daily Practice [ABIDE]), CL was associated with syndromic and etiological diagnosis, with Alzheimer's disease (AD) patients showing the highest amyloid burden, followed by patients with dementia with Lewy bodies (DLB) and patients with cardiovascular disease (CVD). In participants with subjective decline, CL quantification outperformed visual read in predicting global cognitive decline.
3. **Future directions**: This work illustrates the potential value of quantification to optimize the utility of amyloid-PET (positron emission tomography) imaging in the clinical routine, as CL provides information on the presence of primary amyloid or mixed pathology, thereby supporting differential diagnosis in cognitively impaired patients and improves prognostic information in pre-dementia subjects.

cognitively impaired population was on average younger compared to other cohorts. This is because the Alzheimer Centre Amsterdam is a specialized center for cognitive impairment/dementia at a young age.[24] Nonetheless, quantitative amyloid-PET might be of particular value in such cohorts, in line with the appropriate use of criteria.[37] Fourth, using the VR-derived CL cutoff to describe discordance between the two measures is somewhat circular. However, the derived cutoff was identical with that of the AMYPAD DPMS study[36] and highly similar to a [^{18}F]florbetaben PET against post-mortem comparison (i.e., 19 CL). If this latter cutoff would have been implemented, no additional discordant cases would have emerged. Finally, we did not include regional visual assessments, as these were not collected as part of the original study. Although generally omitted for the final classification of amyloid negative or positive, the reader guidelines of [^{18}F]florbetaben include the assessment of four regions of interest, and previous work has illustrated an association between the number of positive regions and CL burden.[6] Thus regional assessments could capture the level of pathology to a certain extent, although a significant reader experience is required. In addition, it has been suggested that spatial distributions could have differential diagnostic and prognostic properties, with posterior amyloid burden more often observed in patients with DLB and associated with worse prognosis in this population.[18] Therefore, spatial distribution might also contribute to distinguishing between patients with DLB and those with emerging AD (i.e., pre-dementia patients) in addition to the clinical phenotype. Because the CL method provides only a global measure of amyloid and considering that the posterior regions are less represented in the standard CL template, it is of interest to further investigate the possible utility of regional VR and regional quantification approaches to optimize clinical amyloid-PET use.

5 | CONCLUSION

In a mixed memory clinic population, we illustrated the potential clinical value of quantification using the CL method. A continuous quantitative measure of amyloid burden provides information on the presence of primary amyloid or mixed pathology, thereby supporting differential diagnosis in cognitively impaired patients and improves prognostic information in pre-dementia subjects. Moreover, with the (future) approval of disease-modifying therapies, amyloid-PET quantitative approaches are becoming increasingly important outside of the research setting. It is, therefore, key to familiarize its users with quantitation in clinical routine.

ACKNOWLEDGMENTS

Research of the Alzheimer Centre Amsterdam is part of the neurodegeneration research program of Amsterdam Neuroscience. The Alzheimer Centre Amsterdam is supported by Stichting Alzheimer Nederland and Stichting VUmc fonds. WMvdF holds the Pasman chair. WMvdF is recipient of the collaboration project ABIDE-clinical utility, which is co-funded by the PPP Allowance made available by health-Holland, Top Sector Life Sciences & Health, to stimulate public-private partnerships and Life Molecular Imaging GmbH (grant no. LSHM18075). WMvdF is recipient of ABOARD, which is a public-private partnership receiving funding from ZonMW (#73305095007), Alzheimer Nederland and Health~Holland, Topsector Life Sciences & Health (PPP-allowance; #LSHM20106). More than 30 partners contribute to ABOARD. ABIDE has been funded in the context of the Dutch national dementia plan (project number: 733050201). The project leading to this article has received funding from the Innovative Medicines Initiative 2 Joint Undertaking under grant agreement No 115952. This Joint Undertaking receives the support from the European Union's Horizon 2020 research and innovation programme and EFPIA. This communication reflects the views of the authors and neither the IMI nor the European Union and EFPIA are liable for any use that may be made of the information contained herein.

CONFLICT OF INTEREST

Lyduine E. Collij has received research support from GE Healthcare (paid to institution). **Gemma** Salvadó reports no relevant disclosures. **Arno** de Wilde is employed by LSP, a life sciences investment firm. **Daniele** Altomare received funding from the Fondation Recherche Alzheimer and the Swiss National Science Foundation (project CRSK-3_196354 / 1). **Mahnaz** Shekari reports no relevant disclosures. **Juan Domingo Gispert** has received speaker's fees from Biogen and Philips. In addition, he holds a "Ramón y Cajal" fellowship (RYC-2013-13054), has received research support from the EU/EFPIA Innovative Medicines Initiative Joint Undertaking AMYPAD grant agreement n° 115952 and from Ministerio de Ciencia y Universidades (grant agreement RTI2018-102261). **Santiago** Bullich is an employee of Life Molecular Imaging GmbH. **Andrew** Stephens is an employee of Life Molecular Imaging GmbH. **Frederik** Barkhof received payment and honoraria from Bayer Genzyme, Biogen-Idec, TEVA, Merck, Novartis, Roche, IXICO Ltd, GeNeuro, and Apitope Ltd for consulting; payment from the IXICOLtd and MedScape for educational presentations; and research support via grants from EU/EFPIA Innovative Medicines Initiative Joint Undertaking (AMYPAD consortium), EuroPOND (H2020), UK MS Society, Dutch MS Society, PICTURE (IMDI-NWO), NIHR UCLH Biomedical Research Centre (BRC), and ECTRIMS-MAGNIMS. **Philip Scheltens** has received consultancy fees (paid to the university) from AC Immune, Alzheon, Brainstorm Cell, ImmunoBrain Checkpoint, Novartis, and Novo Nordisk. Within his university affiliation he is principal investigator of studies with AC Immune, FUJI-film/Toyama, IONIS, UCB, and Vivoryon. He is also an employee of Life Sciences Partners Amsterdam. **Femke Bouwman** has research projects in cooperation with Optina Dx and Optos who paid her institution Alzheimer Center, VU University Medical Center. She has received speaker's fees paid to her institution from Roche and Biogen. **Wiesje M. van der Flier** has research programs that have been funded by ZonMW, NWO, EU-FP7, EU-JPND, Alzheimer Nederland, CardioVascular Onderzoek Nederland, Health~Holland, Topsector Life Sciences & Health, stichting Dioraphte, Gieskes-Strijbis fonds, stichting Equilibrio, Pasman stichting, stichting Alzheimer & Neuropsychiatrie Foundation, Biogen MA Inc, Boehringer Ingelheim, Life-MI, AVID, Roche BV, Fujifilm, and Combinostics, and holds the Pasman chair, is recipient of ABOARD, which is a public-

private partnership receiving funding from ZonMW (#73305095007) and Health~Holland, and Topsector Life Sciences & Health (PPP-allowance; #LSHM20106). In addition, WF has performed contract research for Biogen MA Inc, and Boehringer Ingelheim and has been an invited speaker at Boehringer Ingelheim, Biogen MA Inc, Danone, Eisai, WebMD Neurology (Medscape), and Springer Healthcare. WMvdF is a consultant to Oxford Health Policy Forum CIC, Roche, and Biogen MA Inc. She participated in advisory boards of Biogen MA Inc and Roche. All funding is paid to her institution. WMvdF was associate editor of *Alzheimer, Research & Therapy* in 2020/2021, and is associate editor at *Brain*. Author disclosures are available in the supporting information

REFERENCES

1. Jack CR Jr, Bennett DA, Blennow K, Research Framework NIA-AA. Toward a biological definition of Alzheimer's disease. *Alzheimers Dement*. 2018;14:535-562.
2. Barthel H, Gertz HJ, Dresel S, et al. Cerebral amyloid-beta PET with florbetaben (18F) in patients with Alzheimer's disease and healthy controls: a multicentre phase 2 diagnostic study. *Lancet Neurol*. 2011;10:424-435.
3. de Wilde A, van der Flier WM, Pelkmans W, et al. Association of amyloid positron emission tomography with changes in diagnosis and patient treatment in an unselected memory clinic cohort: the ABIDE Project. *JAMA Neurol*. 2018;75:1062-1070.
4. Rabinovici GD, Gatsonis C, Apgar C, et al. Association of amyloid positron emission tomography with subsequent change in clinical management among medicare beneficiaries with mild cognitive impairment or dementia. *JAMA*. 2019;321:1286-1294.
5. Zwan MD, Bouwman FH, Konijnenberg E, et al. Diagnostic impact of [18F]flutemetamol PET in early-onset dementia. *Alzheimers Res Ther*. 2017;9:2.
6. Collij LE, Salvado G, Shekari M, et al. Visual assessment of [(18)F]flutemetamol PET images can detect early amyloid pathology and grade its extent. *Eur J Nucl Med Mol Imaging*. 2021;48(7):2169-2182.
7. Collij LE, Heeman F, Salvado G, et al. Multitracer model for staging cortical amyloid deposition using PET imaging. *Neurology*. 2020;95:e1538-e1553.
8. Fantoni E, Collij L, Alves IL, Buckley C, Farrar G. The spatial-temporal ordering of amyloid pathology and opportunities for PET imaging. *J Nucl Med*. 2019;61(2):166-171.
9. Mattsson N, Palmqvist S, Stomrud E, Vogel J, Hansson O. Staging β-amyloid pathology with amyloid positron emission tomography. *JAMA neurology*. 2019;76:1319-1329.
10. van der Kall LM, Truong T, Burnham SC, et al. Association of beta-amyloid level, clinical progression and longitudinal cognitive change in normal older individuals. *Neurology*. 2020;96(5):e662-e670.
11. Farrell ME, Chen X, Rundle MM, Chan MY, Wig GS, Park DC. Regional amyloid accumulation and cognitive decline in initially amyloid-negative adults. *Neurology*. 2018;91:e1809-e1821.
12. Farrell ME, Jiang S, Schultz AP, et al. Defining the lowest threshold for amyloid-pet to predict future cognitive decline and amyloid accumulation. *Neurology*. 2021;96:e619-e631.
13. Klunk WE, Koeppe RA, Price JC, et al. The Centiloid Project: standardizing quantitative amyloid plaque estimation by PET. *Alzheimers Dement*. 2015;11:1-15 e11-14.
14. Joie R, Ayakta N, Seeley WW, et al. Multisite study of the relationships between antemortem [(11)C]PIB-PET Centiloid values and postmortem measures of Alzheimer's disease neuropathology. *Alzheimers Dement*. 2018;15(2).
15. Amadoru S, Dore V, McLean CA, et al. Comparison of amyloid PET measured in Centiloid units with neuropathological findings in Alzheimer's disease. *Alzheimers Res Ther*. 2020;12:22.
16. Dore V, Bullich S, Rowe CC, et al. Comparison of (18)F-florbetaben quantification results using the standard Centiloid, MR-based, and MR-less CapAIBL((R)) approaches: validation against histopathology. *Alzheimers Dement*. 2019;15:807-816.
17. Leuzy A, Chiotis K, Hasselbalch SG, et al. Pittsburgh compound B imaging and cerebrospinal fluid amyloid-beta in a multicentre European memory clinic study. *Brain*. 2016;139:2540-2553.
18. Chetelat G, Arbizu J, Barthel H, et al. Amyloid-PET and (18)F-FDG-PET in the diagnostic investigation of Alzheimer's disease and other dementias. *Lancet Neurol*. 2020;19:951-962.
19. Kantarci K, Lowe VJ, Chen Q, et al. beta-Amyloid PET and neuropathology in dementia with Lewy bodies. *Neurology*. 2020;94:e282-e291.
20. Nelson AR, Sweeney MD, Sagare AP, Zlokovic BV. Neurovascular dysfunction and neurodegeneration in dementia and Alzheimer's disease. *Biochim Biophys Acta*. 2016;1862:887-900.
21. Iaccarino L, La Joie R, Koeppe R, et al. rPOP: robust PET-only processing of community acquired heterogeneous amyloid-PET data. *Neuroimage*. 2022;246:118775.
22. Pemberton H, Collij LE, Heeman F, et al. Quantification of amyloid PET for future clinical use: a state-of-the-art review. *J Nucl Med*. 2022;49(10):3508-3528. Accepted.
23. de Wilde A, van Maurik IS, Kunneman M, et al. Alzheimer's biomarkers in daily practice (ABIDE) project: rationale and design. *Alzheimers Dement (Amst)*. 2017;6:143-151.
24. van der Flier WM, Scheltens P. Amsterdam dementia cohort: performing research to optimize care. *J Alzheimers Dis*. 2018;62:1091-1111.
25. Hu Z, Wang W, Gualtieri EE, et al. An LOR-based fully-3D PET image reconstruction using a blob-basis function. *2007 IEEE Nuclear Science Symposium Conference Record*. 2007;6:4415-4418.
26. Youden WJ. Index for rating diagnostic tests. *Cancer*. 1950;3:32-35.
27. Hanseeuw BJ, Malotaux V, Dricot L, et al. Defining a Centiloid scale threshold predicting long-term progression to dementia in patients attending the memory clinic: an [(18)F] flutemetamol amyloid PET study. *Eur J Nucl Med Mol Imaging*. 2020;48(1):302-310.
28. Collij LE, Konijnenberg E, Reimand J, et al. Assessing amyloid pathology in cognitively normal subjects using 18F-flutemetamol PET: comparing visual reads and quantitative methods. *J Nucl Med*. 2019;60:541-547.
29. Thal DR, Beach TG, Zanette M, et al. 18)F]flutemetamol amyloid positron emission tomography in preclinical and symptomatic Alzheimer's disease: specific detection of advanced phases of amyloid-beta pathology. *Alzheimers Dement*. 2015;11:975-985.
30. Lyduine E Collij CB, Palombit A, Gray K, et al. *On behalf of the AMYPAD consortium. Visual assessment and Centiloid quantification across diagnostic groups: the AMYPAD project. EANM*. 2021.
31. Collij LE, Mastenbroek SE, Salvado G, et al. Regional amyloid accumulation predicts memory decline in initially cognitively unimpaired individuals. *Alzheimers Dement (Amst)*. 2021;13:e12216.
32. AHEAD 3-45 Study: A Study to Evaluate Efficacy and Safety of Treatment With BAN2401 in Participants With Preclinical Alzheimer's Disease and Elevated Amyloid and Also in Participants With Early Preclinical Alzheimer's Disease and Intermediate Amyloid [Available from: https://ClinicalTrials.gov/show/NCT04468659

33. Sperling RA, Rentz DM, Johnson KA, et al. The A4 study: stopping AD before symptoms begin? *Sci Transl Med*. 2014;6:228fs213.
34. Cummings J, Aisen P, Apostolova LG, Atri A, Salloway S, Weiner M. Aducanumab: appropriate Use Recommendations. *J Prev Alzheimers Dis*. 2021;8:398-410.
35. Shekari M, Salvadó G, Battle MR, et al. Evaluating robustness of the Centiloid scale against variations in amyloid PET image resolution. *Alzheimer's & Dementia*. 2021;17:e055726.
36. Buckley C, Gispert JD, Altomare D, et al. Quantitative amyloid PET in the AMYPAD diagnostic and patient management study. *Alzheimer's & Dementia*. 2021;17:e055940.
37. Johnson KA, Minoshima S, Bohnen NI, et al. Appropriate use criteria for amyloid PET: a report of the Amyloid Imaging Task Force, the Society of Nuclear Medicine and Molecular Imaging, and the Alzheimer's Association. *J Nucl Med*. 2013;54:476-490.

SUPPORTING INFORMATION

Additional supporting information can be found online in the Supporting Information section at the end of this article.

How to cite this article: Collij LE, Salvadó G, de Wilde A, et al. Quantification of [^{18}F]florbetaben amyloid-PET imaging in a mixed memory clinic population: The ABIDE project. *Alzheimer's Dement*. 2022;00-00.
https://doi.org/10.1002/alz.12886